BNL-211451-2019-JAAM

Removing Cs within a continuous flow set-up by an ionic exchanger material transformable into a final waste form

C. Cabaud, S. Gill

To be published in "Absorption"

March 2019

Nuclear Science and Technology Department

Brookhaven National Laboratory

U.S. Department of Energy

USDOE Office of Science (SC), Nuclear Physics (NP) (SC-26)

DISCLAIMER

Removing Cs within a continuous flow set-up by an ionic exchanger material transformable into a final waste form

Clément Cabaud[1,2] · Yves Barré[1] · Laurent De Windt[2] · Simerjeet Gill[3] · Eric Dooryhée[4] · Mícheál P. Moloney[1,5] · Nicolas Massoni[5] · Agnès Grandjean[1]

Abstract
Silica monoliths loaded with hexacyanoferrate (HCF) nanoparticles were designed and synthesized to selectively remove Cs^+ ions from an aqueous saline solution within a continuous flow set-up. The decontamination and hydrodynamic efficiency of this smart material was compared to other granularly supported HCF. Finally, a thermal treatment was applied to transform the HCF functionalized monolith into a final waste form matrix.

Keywords Ionic exchanger · Monoliths · Continuous flow · Cs decontamination · Densification

1 Introduction

The goal of this study was to develop a monolithic material capable of removing ^{137}Cs from complex radioactive effluents within a closed continuous flow system. This material could then be easily transformed into the final waste form. This material proposed here, which was developed within the framework of hierarchical materials as tailored nuclear waste forms (zur Loye et al. 2018), is a monolithic silica structure with multiscale porosity functionalized by selective Cs-ion exchangers. Once Cs sorption is complete, a high temperature thermal treatment can be then applied to create a dense, and inorganic waste form which traps all the Cs in its silica-based structure.

Among the various suitable ion-exchangers used to selectively remove Cs from radioactive effluents, transition metal hexacyanoferrates (HCF) show attractive properties. These include a high affinity for cesium over a wide range of pH values (Barton et al. 1958; Loos-Neskovic et al. 2004; Nielsen et al. 1987), as well as in the presence of various other competitive ions (Delchet et al. 2012; Lee and Streat 1983; Michel et al. 2017).

Silica monoliths are a new generation of adsorbents with appropriate characteristic lengths and high external surface areas. They are largely used in the field of liquid and gas phase catalysis (Enke et al. 2016). HCF functionalized monoliths contain three pore size domains, all of three of which are intrinsic to this materials' effectiveness. The monolith macropores improve the mass transport to and from the exchange sites when compared to packed beds for an in-flow removal process. The mesopores provide a hard template for the growth of HCF particles. Lastly, the size of the micropores corresponds to the K^+ loaded internal channels of HCF lattice structure. In addition to their porosity, these large cylindrical objects are easier to handle than powder form solids avoiding the risk of dispersion while optimizing the filling of packages for nuclear waste storage. Up to now, all in-flow experiments described in the literature where Cs is extracted from contaminated effluents have been performed using grain-filled columns (Michel et al. 2018;

Electronic supplementary material The online version of this article (https://doi.org/10.1007/s10450-019-00040-6) contains supplementary material, which is available to authorized users.

✉ Agnès Grandjean
agnes.grandjean@cea.fr

1 CEA, DEN, DE2D, SEAD, Laboratory of Supercritical and Decontamination Processes, Univ. Montpellier, 30207 Bagnols-sur-Cèze, France

2 MINES Paris Tech, PSL University, Centre de Géosciences, 77300 Fontainebleau, France

3 Nuclear Science and Technology Department, Brookhaven National Lab, Upton, NY 11973, USA

4 Photon Division, Brookhaven National Lab, Upton, NY 11973, USA

5 CEA, DEN, DE2D, SEVT, Research Laboratory for the Development of Conditioning Matrices, Univ. Montpellier, 30207 Bagnols-sur-Cèze, France

Milonjic et al. 2002; Mimura et al. 1999a, b, 2007; Novosad et al. 1992; Vincent et al. 2014a). While the literature does report certain monolithic materials which are able to extract Cs in batch mode (Causse et al. 2014), to the best of our knowledge there has been nothing reported on their use in continuous flow mode experiments.

R&D on the treatment of contaminated liquid wastes is normally approached as it they are two isolated topics. The first consist of the selective transfer of the Cs from the liquid phase to a solid phase, while the second focuses on the development of a containment matrix that matches the solid phase prepared in step one. In this communication we hope to bridge this disconnect. Similarly, the management of radioactive solid waste is hardly ever mentioned in relation to pure zeolite materials (Aono et al. 2018; Bosch et al. 2004; Brundu and Cerri 2015; Liguori et al. 2013) or hybrid adsorbent (Yin et al. 2014; Zhang et al. 2017). Also, the direct conversion of HCF loaded silica materials used in the continuous flow Cs removal from a contaminated effluent has never been reported before.

2 Results and discussion

2.1 Synthesis

The silica monolith was synthesized by a sol–gel method coupled with a spinodal decomposition (Nakanishi 1997) in which a tetraethoxysilane (TEOS) solution was mixed with an organic polymer (polyoxyethylene, PEO) over 3 days at 40 °C to control the macroporosity. The second stage of the synthesis was an alkaline treatment leading to a disordered mesoporosity via an Ostwald ripening phenomena (Babin et al. 2007; Galarneau et al. 2016a, b). Eventually, washing and calcination at 550 °C in air for 6 h led to a centimeter-scale monolithic sample. The monolith was then placed in a plastic heat shrink sleeve with connectors at both ends. The functionalisation was carried out under flow through the column with a modified experimental protocol reported for use on silica grains (Michel et al. 2017). The first step consisted of an alkaline pretreatment using a 10^{-4} mol L^{-1} aqueous KOH solution (pH 10). HCF nanoparticles were then grown within the pores using a two-step addition process. Typically, 40 mL of a 10^{-2} mol L^{-1} copper nitrate solution was passed through the monolith (length = 3 cm; diameter = 0.9 cm; weight = 0.5 g) for 20 min. The monolith was then washed with deionized water to remove any excess copper. 40 mL of a mixed 10^{-2} mol L^{-1} $K_4Fe(CN)_6/KNO_3$ solution was percolated through the monolith for 20 min. The now HCF functionalized monolith (named Cu-HCF@silica-monolith) is then washed one final time with deionized water (Fig. 1).

2.2 Structural and textural characterization

The hierarchical pores structure of the monolith was observed by SEM and TEM 15 µm macropores where observed by SEM (Fig. 1). An analysis by mercury intrusion confirmed the presence of macropores with median pore diameter of 9 µm (Fig. S1a, Electronic Supported Information (ESI)). Observation by SEM and TEM indicated the presence a two populations of HCF particles. SEM

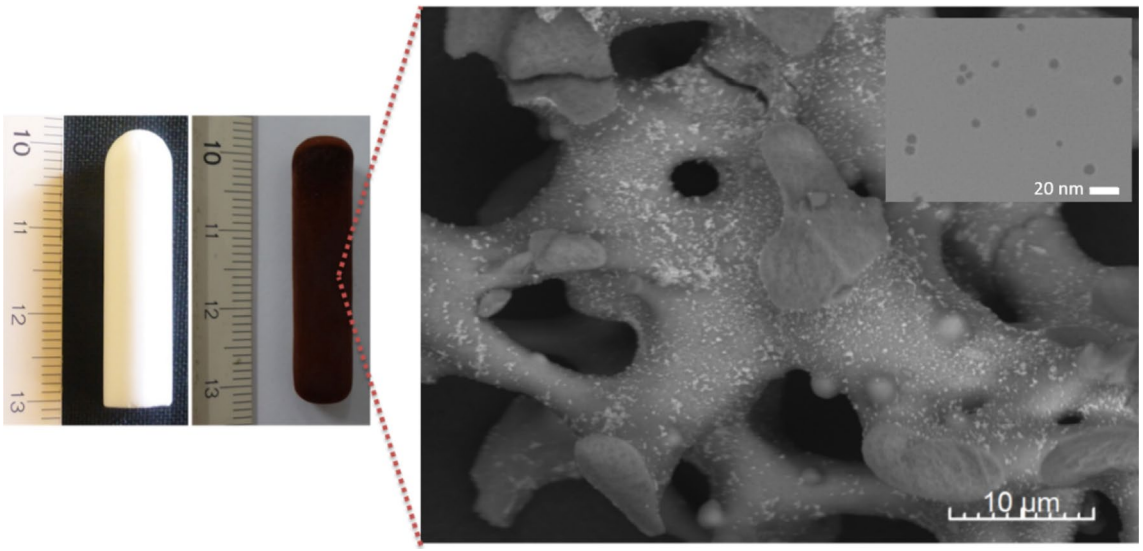

Fig. 1 Left: Photographs of monoliths before (white) and after (black) functionalisation with HCF particles. Right: SEM picture of the crushed Cu-HCF@silica-monolith showing the macroporosity and spots of HCF all over the skeleton; in the top insert: TEM picture showing the nanoparticles

showed the presence of large particles or aggregates, with size around 100 nm all over the surface of macropores. TEM (Fig. 1) also indicated the presence of 5–10 nm HCF nanoparticles corresponding to the size range of the mesopores in which they were grown.

The nitrogen adsorption isotherm of pristine sample showed a type IVa hysteresis loop which is characteristic of mesoporous structure (Fig. S1b). Growth of Cu-HCF particles leads to a 53.6% decrease of the specific surface (from 725 to 336 $m^2\ g^{-1}$ for pristine and loaded material, respectively). A partial clogging of the pore volume and consequent reduction in pore volume (from 1.08 to 0.77 $cm^3\ g^{-1}$ at $P/P_0 = 1$ for pristine and loaded material, respectively) is the probable cause of it.

X-ray diffraction measurements were performed at X-ray Powder Diffraction (XPD) beamline at NSLS II. Samples were mounted in Kapton capillaries and measurements were done in transmission mode using Silicon-base flat panel detector (for details see SI). XRD patterns of both the Cu-HCF@silica-monolith, as well as a control material, a template-less classically precipitated Cu-HCF, show well defined reflections confirming the crystalline nature of these materials, (see in Fig. S2, ESI). All the Cu-HCF materials are found to possess a face centered cubic structure with Fm-3m symmetry, as well as a minor impurity phase(s), (Fig. S3, ESI). This is in agreement with previously reported Cu-HCF studies (Ojwang et al. 2016; Wardecki et al. 2017).

2.3 Sorption properties

The main sorption properties were obtained in batch mode by immersing 100 mg of crushed monolith in 100 mL of commercially available mineral water (the composition is given in Table S1, ESI) of different Cs concentrations. The Cs concentration in the isotherm sorption tests range from trace concentration (10^{-10} mol L^{-1}) using ^{137}Cs, to 10^{-3} mol L^{-1} using ^{133}Cs. The maximum sorption capacity of the crushed monolith, (Fig. 2a), is close to the capacity of silica grains loaded with the same kind of Cu-HCF (Michel et al. 2018, 2017) i.e. 0.058 and 0.063 mmol of Cs per gram of material, respectively. This means that the amounts of HCF are similar in both cases (in between 3 and 4 wt% according to elemental analysis of silica grains). This HCF concentration was confirmed by elemental analyses of the Cu-HCF@monolith giving a composition of 2.6 wt% with HCF and a molar ratio of Cu/Fe = 1.51. Assuming $K_{2x}Cu_{2-x}Fe(CN)_6$ structure of Cu-HCF particles (Letho et al. 1990) gives x = 0.49 and a theoretical maximum sorption equal to 0.064 mmol g^{-1} close to the experimental maximum sorption capacity. This low HCF concentration leads to a maximum sorption capacity in the lower range of published HCF-supported materials (see Table 8 in. (Alby et al. 2018)).

However, for trace concentration and continuous flow use, the key factors are the rate of sorption and the distribution coefficient (K_d).

The kinetics experiment was performed with 50 mg L^{-1} of ^{133}Cs, showing that 94% of the Cs capacity was reached after only one minute (Fig. 2b). Full equilibrium required 5 min. The K_d of the crushed monolith reaches 5×10^5 mL g^{-1}. The comparison of these results with the large amount of available literature data on HCFs of various transition metals (Cu, Co, Zn, Ni) and loaded onto various (organic, or inorganic) supports is relatively tricky due to different experimental conditions (Delchet et al. 2012; Ishfaq et al. 1993; Lee and Streat 1983; Letho and Szirtes 1994; Michel et al. 2017; Mimura et al. 1998a, b, 1997; Nilchi et al. 2006; Orechovska and Rajec 1999; Shahbandeh and Streat 1982; Turgis et al. 2013; Vincent et al. 2014b; Wang et al. 2009). The Cu-HCF@silica-monolith reported here exhibits one of the fastest kinetics (Olatunji et al. 2015) and a Kd in the upper range of results published for loaded HCF materials. With the same experimental conditions, silica grains obtained by a similar process (Michel et al. 2017) or monolith synthesized in a one-pot process (Causse et al. 2014) show a lower Kd, while equilibrium was reached after several hours for bulk-HCF (Delchet et al. 2012) and more than 5 days for Ni-HCF loaded onto dense $Zr(OH)_4$ grains (Michel et al. 2015).

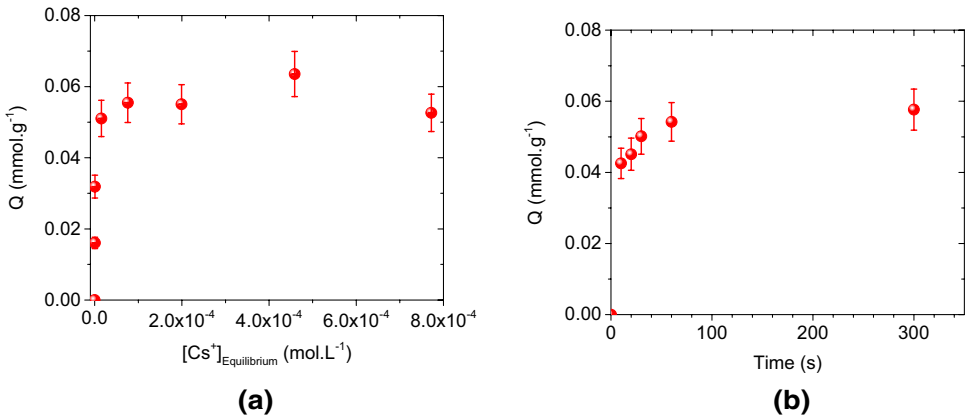

Fig. 2 **a** Sorption isotherm of Cs for crushed monolith in freshwater; **b** Kinetics of Cs sorption on crushed silica monolith in freshwater ([Cs+] $i = 3.9 \times 10^{-4}$ mol L^{-1})

XRD patterns (Fig. S2, ESI) show that lattice parameter "a" increases for both bulk and silica loaded nano Cu-HCF's from ~10.03 to 10.1 Å (Table S2, ESI) after Cs sorption. Such expansion of lattice when intercalated K^+ is exchanged with Cs^+ is previously reported (Renman et al. 2017; Steen et al. 2002) suggesting changes in the local chemical structure that could explain the high Cs selectivity.

In a series of breakthrough experiments, the Cs-doped mineral water percolated within the monolith itself. The setup used for the breakthrough curve experiments is described in SI (Fig. S4). The Cs-containing solution was injected into the column using a peristaltic pump. The column flow-through effluents were collected in 8 mL fractions with an automatic fraction collector, and then analyzed by Atomic Absorption. The sorption capacity, the selectivity, the sorption rate, the column inlet concentration, the inlet flow, all play a key role during the dynamic sorption process and affect the shape of the breakthrough curve. The silica monolith was compared to other HCF functionalized inorganic packed grains supports having a grain size between 300 and 500 µm. These included (i) crushed Cu-HCF@silica-monolith, (ii) packed grains of Cu-HCF loaded on mesoporous silica (Cu-HCF@silica-grains) and (iii) packed grains of Ni-HCF loaded on a dense $Zr(OH)_4$ support (Ni-HCF@zirconia). The shape of the column and the bed volume were identical for all the breakthrough experiments. These in-flow experiments were performed at a high amount of Cs (2.5×10^{-4} mol L^{-1}), compared to actual effluents with trace concentrations of ^{137}Cs, to reduce the duration of the experiments. The curves were normalized with respect to the half breakthrough volume (Fig. 3). In all case, the first percolating volumes contain a small fraction of Cs ($C/C_0 < 0.1$) due to a release of poorly-fixed HCF nanoparticles in the outflow. Each column was washed with deionized water before starting the control. However, the increase of ionic strength in the presence of mineral water and cesium nitrate modifies the ζ-potential and aggregate size (Dedovets et al. 2016) and this could explain this preliminary expulsion of some nanoparticles under flow. Afterwards, the Cs concentration remained very low until the full breakthrough took place.

An indicator of the efficiency of the fixed bed to extract Cs under flow can be defined as following (Rojas-Mayorga et al. 2015):

$$Bed\ Efficiency = \frac{\int_{V=0}^{V_R} [Cs]_i - [Cs]_{outlet}\, dV}{V_R [Cs]_i}$$

where $[Cs]_i$ and $[Cs]_{outlet}$ are the concentration of Cs at the inlet and the outlet of the column respectively, Vr is the volume necessary to obtain the concentration at the outlet of the column equal to half of the concentration at the inlet of the column. This parameter corresponds to the fraction (in %) of Cs adsorbed by the solid materials under flow versus the total amount of Cs that percolated through the column at mid-breakthrough. The higher the Bed Efficiency (BE) is, the steeper is the breakthrough curve, and the more efficient is the decontamination process.

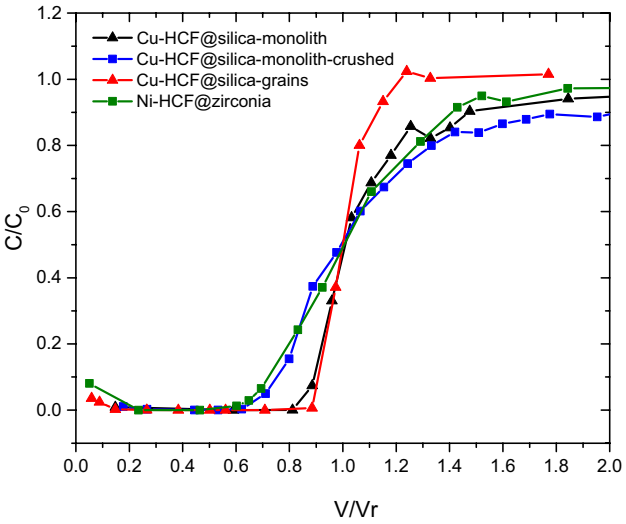

Fig. 3 Comparison of normalized Cs breakthrough curves in continuous flow (Darcy/linear velocity = 1 m h^{-1}; $C_0 = 2.5\times10^{-4}$ mol L^{-1}) for Cu-HCF@silica-monolith (black), packed Cu-HCF@silica-monolith-crushed (blue), Cu-HCF@silica-grains (red) and dense Ni-HCF@zirconia (green)

The Cu-HCF@silica-grains bed gives the steepest breakthrough and the highest BE (96%). The Cu-HCF@silica-monolith is also very steep up to the breakthrough point, but then becomes less efficient, corresponding to a slightly lower BE (91%). The shape of the second part of the breakthrough may be due to the existence of less accessible zones of the skeleton where pores clogging or HCF aggregation, as suggested by SEM, hampers mass transfer efficiency.

The crushed Cu-HCF@silica-monolith has a broader breakthrough profile and lower BE (83%) than the initial monolith. This is due to preferential flow between grains at the expense of diffusion into the macro and meso-porosities of the grains where the Cu-HFC are mostly located. The use of a dense support leads to widespread breakthrough profile for Ni-HCF@zirconia and a low BE (76%), again due to a competition between inter-grain flow and intra-grain diffusion (Michel et al. 2015, 2017).

2.4 Densification by thermal treatment

The last step of the present study concerns the direct (means with limited operations) transformation of Cs-loaded Cu-HCF@silica-monolith into the waste form. The monoliths themselves cannot be used as a waste form because they are porous. The objective here is to show that it could possible

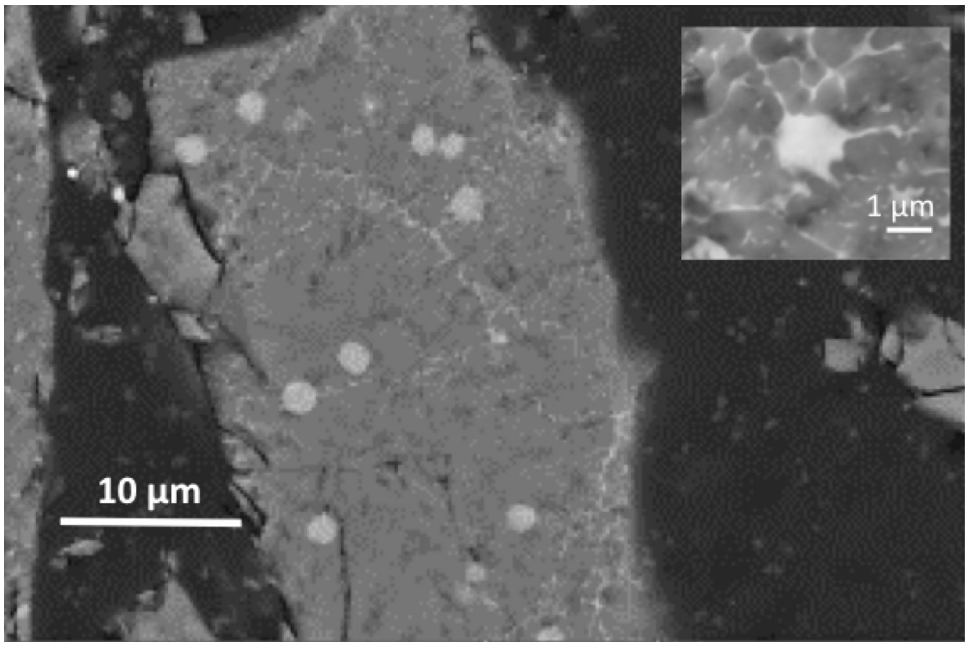

Fig. 4 SEM picture of the Cu-HCF@silica-beads after annealing at 1000 °C

to densify the monoliths with the lowest Cs loss as possible. Similar radioactive silica-based sorbents can be converted into a dense waste form by a thermal treatment (Wu et al. 2018; Zhang et al. 2017), eventually with addition of other compounds to limit Cs loss (Yin et al. 2014). Cementation is a low cost technique but it means higher volumes due to usual low loading factor. Hence, the ability of a thermal treatment to close the porosity of functionalized silica raw material without additives was seen as an optimal densification route for this kind of monolithic sorbent. Air annealing's of Cu-HCF@silica-beads were performed from 100 °C to 1000 °C with a maximal mass loss of 7.3% measured at 1000 °C. The Cu-HCF degradation begins between 150 °C and 250 °C depending on the composition and Cs content as expected from pure-Cu-HCF studies and according to infrared analysis (Fig S5, ESI) (Åkerblom et al. 2017). Cu-HCF@silica exhibits about the same behavior with the total degradation of Cu-HCF at temperature higher than 300 °C as detected by XRD. The sample remains mainly amorphous up to 800 °C, but crystallization of cristobalite is observed at 900 °C. The SEM observation (Fig. 4) shows the presence of Cs–K–Cu–Fe–Si–O dots (white inclusions) suggesting a strong interaction between Cu, Fe, K, Cs (from HCF) and silica, explaining Cs retention.

A phase analogous to pollucite $CsAlSi_2O_6$ with Al substituted by Fe is a hypothesis that is currently investigated. This phenomenon was also observed with Co-HCF and Ni-HCF zeolites (Ikarashi et al. 2014). The comparison of elemental analyses of the unheated sample and the sample heated at 1000 °C confirms the absence of Cs loss during heating (Table S3, ESI). The annealed sample did not stick and densify but a supplementary beneficial aspect is that both the total pore volume and BET specific surface drastically decreased, i.e. from 0.722 $cm^3\ g^{-1}$ and 140.4 $m^2\ g^{-1}$ for unheated material to 0.021 $cm^3\ g^{-1}$ and 0.75 $m^2\ g^{-1}$ for the 1000 °C-annealed one. Indeed, after the encapsulation treatment, the nitrogen adsorption isotherm curve is flat without hysteresis, meaning the closure of the mesoporosity (Fig. S1b, ESI). The fact that HCF has decomposed, silica pores collapsed and Cs did not volatilize with a single oxidic treatment is a positive basis for a dense, chemically stable and durable waste form.

3 Conclusion

In summary, we propose the synthesis of Cu-HCF loaded silica monoliths suitable for the removal of contaminate Cs from radioactive aqueous solutions. These monolithic materials are very promising for in-flow process compared to other competitive sorbents due to their fast sorption kinetics and their hierarchical porosity. Furthermore, these materials present high distribution coefficients using radioactive ^{137}Cs, even in presence of competitive cations such Na^+, Mg^{2+} and Ca^{2+} (mineral water), as well as high bed efficiency under flow. Finally, thermal treatment of Cu-HCF@silica-monolith leads to closure of the porosity without volatilization of Cs. These properties are crucial in the field of continuous process of saline wastewater decontamination and management of final waste form.

Acknowledgements Research was conducted in part by the Center for Hierarchical Waste Form Materials (CHWM), an Energy Frontier Research Center (EFRC) supported by the U.S. Department of Energy,

Office of Basic Energy Sciences, Division of Materials Sciences and Engineering under Award DE-SC0016574. A part of this research used resources of XPD beamline of the National Synchrotron Light Source II, a U.S. Department of Energy (DOE) Office of Science User Facility operated for the DOE Office of Science by Brookhaven National Laboratory under Contract No. DE-SC0012704. We also thank the EDDEM-CEA Project for funding this work, and Virginie Fremy for aqueous sample analysis, and Lionel Campayo for fruitful discussion.

References

Åkerblom, I.E., Ojwang, D.O., Grins, J., Svensson, G.: A thermogravimetric study of thermal dehydration of copper hexacyanoferrate by means of model-free kinetic analysis. J. Therm. Anal. Calorim. **129**, 721–731 (2017). https://doi.org/10.1007/s10973-017-6280-x

Alby, D., Charnay, C., Heran, M., Prelot, B., Zajac, J.: Recent developments in nanostructured inorganic materials for sorption of cesium and strontium: synthesis and shaping, sorption capacity, mechanisms, and selectivity—a review. J. Hazard. Mater. **344**, 511–530 (2018). https://doi.org/10.1016/j.jhazmat.2017.10.047

Aono, H., Takahashi, R., Itagaki, Y., Johan, E., Matsue, N.: Cs immobilization using the formation of the glassy phase by the heat-treatment of natural mordenite. J. Nucl. Mater. **508**, 20–25 (2018). https://doi.org/10.1016/j.jnucmat.2018.05.027

Babin, J., Iapichella, J., Lefèvre, B., Biolley, C., Bellat, J.-P., Fajula, F., Galarneau, A.: (2007) MCM-41 silica monoliths with independent control of meso- and macroporosity New J. Chem. **31**, 1907 https://doi.org/10.1039/b711544j

Barton, G.B., Hepworth, J.L., McClanahan, E.D., RLM, J., Tuyl, H.H.V.: Chemical processing wastes. Recover. Fission Prod. Ind. Eng. Chem. **50**, 212–216 (1958)

Bosch, P., Caputo, D., Liguori, B., Colella, C.: Safe trapping of Cs in heat-treated zeolite matrices. J. Nucl. Mater. **324**, 183–188 (2004). https://doi.org/10.1016/j.jnucmat.2003.10.001

Brundu, A., Cerri, G.: Thermal transformation of Cs-clinoptilolite to $CsAlSi_5O_{12}$. Microporous Mesoporous Mater. **208**, 44–49 (2015). https://doi.org/10.1016/j.micromeso.2015.01.029

Causse, J., Tokarev, A., Ravaux, J., Moloney, M., Barré, Y., Grandjean, A.: Facile one-pot synthesis of copper hexacyanoferrate nanoparticle functionalised silica monoliths for the selective entrapment of ^{137}Cs. J. Mater. Chem. A. **2**, 9461 (2014). https://doi.org/10.1039/c4ta01266f

Dedovets, D., Bauduin, P., Causse, J., Girard, L., Diat, O.: Switchable self-assembly of Prussian blue analogs nano-tiles triggered by salt stimulus. Phys. Chem. Chem. Phys. **18**, 3188–3196 (2016). https://doi.org/10.1039/c5cp06574g

Delchet, C., et al.: Extraction of radioactive cesium using innovative functionalized porous materials. RSC Adv. **2**, 5707 (2012). https://doi.org/10.1039/c2ra00012a

Enke, D., Gläser, R., Tallarek, U.: Sol–gel and porous glass-based silica monoliths with hierarchical pore structure for solid–liquid catalysis. Chem. Ing. Tec. **88**, 1561–1585 (2016). https://doi.org/10.1002/cite.201600049

Galarneau, A., et al.: Synthesis and textural characterization of mesoporous and meso-/macroporous silica monoliths obtained by spinodal decomposition. Inorganics. **4**, 9 (2016a). https://doi.org/10.3390/inorganics4020009

Galarneau, A., et al.: Hierarchical porous silica monoliths: a novel class of microreactors for process intensification in catalysis and adsorption. C. R. Chim. **19**, 231–247 (2016b). https://doi.org/10.1016/j.crci.2015.05.017

Ikarashi, Y., et al.: (2014) Selective adsorption properties and stable solification of Cs by insoluble ferrocyande loaded zeolites. In: Proceedings of the Paper presented at the 21st International Conference on Nuclear Engineering – 2013, Vol 5, V005T08A005, New York

Ishfaq, M.M., Karim, H.M.A., Khan, M.A.: Adsorptions studies of cesium on potassium copper nickel hexacyanoferrate(II) from aqueous solutions. J. Radioanal. Nucl. Chem. **170**, 321–331 (1993)

Lee, E.F.T., Streat, M.: Sorption of ceasium by complex hexacyanoferrates III. A study of the sorption properties of potassiupm copper ferrocyanide. J. Chem. Technol. Biotechnol. **33**, 80–86 (1983)

Letho, J., Szirtes, L.: Mechanism of caesium ion exchange on potassium cobalt hexacyanoferrates(II) ion exchangers radiations. Phys. Chem. **43**, 261–264 (1994)

Letho, J., Haukka, S., Harjula, R.: (1990) Mechanism of caesium ion exchange on potassium cobalt hexacyanoferrates(II). Dalton Trans. **3**, 1007–1011

Liguori, B., Caputo, D., Iucolano, F., Aprea, P., de Gennaro, B.: Entrapping of Cs and Sr in heat-treated zeolite matrices. J. Nucl. Mater. **435**, 196–201 (2013). https://doi.org/10.1016/j.j.nucmat.2012.12.043

Loos-Neskovic, C., et al.: Structure of copper-potassium hexacyanoferrate (II) and sorption mechanisms of cesium. J. Solid State Chem. **177**, 1817–1828 (2004). https://doi.org/10.1016/j.jssc.2004.01.018

Michel, C., Barré, Y., de Dieuleveult, C., Grandjean, A., De Windt, L.: Cs ion exchange by a potassium nickel hexacyanoferrate loaded on a granular support. Chem. Eng. Sci. **137**, 904–913 (2015). https://doi.org/10.1016/j.ces.2015.07.043

Michel, C., Barré, Y., De Windt, L., de Dieuleveult, C., Brackx, E., Grandjean, A.: Ion exchange and structural properties of a new cyanoferrate mesoporous silica material for Cs removal from natural saline waters. J. Environ. Chem. Eng. **5**, 810–817 (2017). https://doi.org/10.1016/j.jece.2016.12.033

Michel, C., Barré, Y., Ben Guiza, M., de Dieuleveult, C., De Windt, L., Grandjean, A.: Breakthrough studies of the adsorption of Cs from freshwater using a mesoporous silica material containing ferrocyanide. Chem. Eng. J. **339**, 288–295 (2018). https://doi.org/10.1016/j.cej.2018.01.101

Milonjic, S., Bispo, I., Fedoroff, M., Loos-Neskovic, C., Vidal-Madjarc, C.: Sorption of cesium on copper hexacyanoferrate/polymer/silica composites in batch and dynamic conditions. J. Radioanal. Nucl. Chem. **252**, 497–501 (2002)

Mimura, H., Lehto, J., Harjula, R.: Ion exchange of cesium on potassium nickel hexacyanoferrate IIs. J. Nucl. Sci. Technol. **34**, 484–489 (1997). https://doi.org/10.1080/18811248.1997.9733695

Mimura, H., Kageyama, N., Akiba, K., Yoneya, M., Miyamoto, Y.: Ion-exchange properties of potassium nickel hexacyanoferrate(II) Compounds. Solvent Extr. Ion Exchange. **16**, 1013–1031 (1998a). https://doi.org/10.1080/07366299808934566

Mimura, H., Kimura, M., Akiba, K., Onodera, Y.: Physicochemical properties of potassium nickel hexacyanoferrate(II)-loaded chabazites. J. Nucl. Sci. Technol. **35**, 392–395 (1998b). https://doi.org/10.1080/18811248.1998.9733876

Mimura, H., Kimura, M., Akiba, K., Onodera, Y.: Selective REMOVAL of cesium from sodium nitrate solutions by potassium nickel hexacyanoferrate-loaded chabazites separation. Sci. Technol. **34**, 17–28 (1999a). https://doi.org/10.1081/ss-100100633

Mimura, H., Kimura, M., Akiba, K., Onodera, Y.: Separation of cesium and strontium by potassium nickel. J. Nucl. Sci. Technol. **36**, 307–310 (1999b). https://doi.org/10.1080/18811248.1999.9726213

Mimura, H., Kimura, M., Akiba, K., Onodera, Y.: Selective removal of cesium from highly concentrated sodium nitrate neutral solutions by potassium nickel hexacyanoferrate(II)-loaded silica gels. Solvent Extract Ion Exch. **17**, 403–417 (2007). https://doi.org/10.1080/07366299908934620

Nakanishi, K.: (1997) Pore structure control of silica gels based on phase separation. J. Porous Mater. **4**, 67–112

Nielsen, P., Dresow, B., Heinrich, H.C.: In vitro Study of 137Cs sorption by hexacyanoferrates(II). J. Chem. Sci. **42**, 1451–1460 (1987)
Nilchi, A., Khanchi, A., Atashi, H., Bagheri, A., Nematollahi, L.: The application and properties of composite sorbents of inorganic ion exchangers and polyacrylonitrile binding matrix. J. Hazard. Mater. **137**, 1271–1276 (2006). https://doi.org/10.1016/j.jhazmat.2006.04.043
Novosad, J., Jandl, J., Woollins, J.D.: Characterization of modified clinoptilolite. J. Radioanal. Nucl. Chem. **165**, 287–294 (1992). https://doi.org/10.1007/bf02166146
Ojwang, D.O., et al.: Structure characterization and properties of K-containing copper. Hexacyanoferrate Inorg. Chem. **55**, 5924–5934 (2016). https://doi.org/10.1021/acs.inorgchem.6b00227
Olatunji, M.A., Khandaker, M.U., Mahmud, H.N.M.E., Amin, Y.M.: Influence of adsorption parameters on cesium uptake from aqueous solutions- a brief review. RSC Adv. **5**, 71658–71683 (2015). https://doi.org/10.1039/c5ra10598f
Orechovska, J., Rajec, P.: Sorption of cesium on composite sorbents based on nickel ferrocyanide. J. Radioanal. Nucl. Chem. **242**, 387–390 (1999)
Renman, V., Ojwang, D.O., Valvo, M., Gomez, C.P., Gustafsson, T., Svensson, G.: Structural-electrochemical relations in the aqueous copper hexacyanoferrate-zinc system examined by synchrotron X-ray diffraction. J. Power Sources. **369**, 146–153 (2017). https://doi.org/10.1016/j.jpowsour.2017.09.079
Rojas-Mayorga, C.K., Bonilla-Petriciolet, A., Sánchez-Ruiz, F.J., Moreno-Pérez, J., Reynel-Ávila, H.E., Aguayo-Villarreal, I.A., Mendoza-Castillo, D.I.: Breakthrough curve modeling of liquid-phase adsorption of fluoride ions on aluminum-doped bone char using micro-columns: Effectiveness of data fitting approaches. J. Mol. Liq. **208**, 114–121 (2015). https://doi.org/10.1016/j.molliq.2015.04.045
Shahbandeh, M.R., Streat, M.: Sorption of caesium by complex hexacyanoferrates: I. Sorption and physical properties of sodium-copper cyanoferrates (II). J. Chem. Technol. Biotechnol. **32**, 580–585 (1982)
Steen, W.A., et al.: Structure of cathodically deposited nickel hexacyanoferrate thin films using XRD and EXAFS. Langmuir. **18**, 7714–7721 (2002). https://doi.org/10.1021/la020352e
Turgis, R., et al.: An original "Click and Bind" approach for immobilizing copper hexacyanoferrate nanoparticles on mesoporous silica. Chem. Mater. **25**, 4447–4453 (2013). https://doi.org/10.1021/cm4029935
Vincent, C., Hertz, A., Vincent, T., Barré, Y., Guibal, E.: Immobilization of inorganic ion-exchanger into biopolymer foams—application to cesium sorption. Chem. Eng. J. **236**, 202–211 (2014a). https://doi.org/10.1016/j.cej.2013.09.087
Vincent, T., Vincent, C., Barré, Y., Guari, Y., Le Saout, G., Guibal, E.: Immobilization of metal hexacyanoferrates in chitin beads for cesium sorption: synthesis and characterization. J. Mater. Chem. A. **2**, 10007 (2014b). https://doi.org/10.1039/c4ta01128g
Wang, L., et al.: Supporting of potassium copper hexacyanoferrate on porous activated carbon substrate for cesium separation separation. Sci. Technol.. **44**, 4023–4035 (2009). https://doi.org/10.1080/01496390903183253
Wardecki, D., Ojwang, D.O., Grins, J., Svensson, G.: Neutron diffraction and EXAFS studies of $K_{2x}/_3Cu[Fe(CN)_6]_{2/3}{\cdot}nH_2O$ Crystal. Growth Des. **17**, 1285–1292 (2017). https://doi.org/10.1021/acs.cgd.6b01684
Wu, Y., Lee, C.-P., Mimura, H., Zhang, X., Wei, Y.: Stable solidification of silica-based ammonium molybdophosphate by allophane: application to treatment of radioactive cesium in secondary solid wastes generated from fukushima. J. Hazard. Mater. **341**, 46–54 (2018). https://doi.org/10.1016/j.jhazmat.2017.07.044
Yin, X., Wu, Y., Mimura, H., Niibori, Y., Wei, Y.: Selective adsorption and stable solidification of radioactive cesium ions by porous silica gels loaded with insoluble ferrocyanides. Sci. China Chem. **57**, 1470–1476 (2014). https://doi.org/10.1007/s11426-014-5211-y
Zhang, X., Wu, Y., Wei, Y., Mimura, H., Matsukura, M.: Stable solidification of cesium with an allophane additive by a pressing/sintering method. J. Nucl. Mater. **485**, 39–46 (2017). https://doi.org/10.1016/j.jnucmat.2016.12.029
zur Loye, H.-C., et al.: (2018) Hierarchical materials as tailored nuclear waste forms: a perspective. Chem. Mater. https://doi.org/10.1021/acs.chemmater.8b00766